Journal of Scientific & Industrial Research
Vol. 81, February 2022, pp. 188-201

A Dynamic Image Analysis Method for Fragmentation Measurement in Blasting

Lalit Singh Chouhan[1]*, A K Raina[2] and V M S R Murthy[3]

[1]Mining Department, Kotputli Cement Work, UltraTech Cement Limited, Jaipur, India

[2]CSIR-Central Institute of Mining and Fuel research, Nagpur, India

[3]Department of Mining Engineering, Indian Institute of Technology (Indian School of Mines), Dhanbad 826 004, India

Received 14 September 2021; revised 16 January 2022; accepted 17 January 2022

Fragment size optimization with selection of best values of blast design variables is an important process in mine-mill fragmentation system to maximize the system performance. This calls for measurement and analysis of mean fragment size with respect to blast design parameters. Digital image analysis technique is the most accepted method for measurement of blasted fragment sizes and their distribution. For quick assessment of the fragment sizes, a new novel method based on the digital images extracted from a blast video is reported in this paper. Correction factor for the size of fragments, considering the face movement is also proposed. The method has been tested with the help of seven blast data sets. The proposed dynamic image analysis technique can not only be used in fragment size estimation but also to assess the time-progressive size reduction in a blast, which can help designing the delay timing. Further, a possibility to estimate the in-situ block size is also explored with this method. The images of blast fragmentation were extracted from their videos at an interval of 0.08 s. These images were analyzed later for measurement of mean fragment size at respective times. The fragment size of the complete muck generated by the blast was also measured and correlated well with the sizes achieved from video analysis. The analysis revealed that from 0.08 s to 0.56 s from the initiation of the blasts, the fragment size reduction progressed from 58% to 80% of the estimated in-situ rock block sizes. Significant effect of blast design variables and two firing patterns on the mean fragment size was also observed. The analysis suggested that V-type firing pattern provides finer fragment size in comparison to the diagonal firing pattern. The suggested method provides an easy yet fast way for the assessment of blast fragment size.

Keywords: Blasting, Blast Design, Dynamic image analysis, Fragmentation

Symbols and Abbreviations

H_b	Bench height (m)	B	Burden (m)	Be	Effective burden (m)
S	Spacing (m)	Se	Effective spacing (m)	ls	Stemming length (m)
k_{50}	Mean fragment size (m)	d	Blasthole diameter(mm)	q	Specific charge (kg/m^3)
Q	Explosive charge per hole (kg)	FP	Firing pattern	q	Specific charge
k_{50} v	Mean fragment size obtained from video image analysis	DIAT	Digital image analysis technique	k_{50B}	Overall mean fragment size obtained from blast
k_{opt}	Optimum fragment size (all in m)			k_{50C}	Corrected k_{50V}

Introduction

Fragmentation is one of the most important concepts in explosives engineering. Blasting is the first step of the size reduction of the in-situ rock mass in mining and is followed by crushing and grinding operations and is a part of the Mine-Mill Fragmentation System (MMFS). Rock fragmentation by blasting is the first stage of the comminution process in mines and has the maximum leverage in the efficiency of a mining operation, as the output from a blast impacts every downstream operation.[1] The cost equations of different unit operations of the MMFS[2] are conflicting in nature.[3] Hence, cost minimization of the system cannot be achieved, and optimization is the only option. Since, the efficiency of these unit operations is directly related to the fragment size distribution of muck pile, the outcome of a good blasting operation leads to the productiveness of the next stages of mining, such as loading, hauling and crushing processes.[4,5] Accordingly, the efficiency of a blasting operation is determined by matching the fragment size achieved in blasting with the required one.

Drilling and blasting cost in open pit mines constitutes around 15% to 20% of the total mining

*Author for Correspondence
E-mail: chouhan4569@gmail.com

cost.[6–8] Apart from the direct costs, blasting efficiency also influences down the line mining costs, that account for 80–85% of the mining cost.[2] The cost equation therefore requires a focus on achieving the optimum fragment size in blasting which in turn will result in optimum performance of the MMFS. The required specifications or optimum fragment size (k_{opt}) are usually governed by the loading and hauling equipment, and importantly, the primary crushing units.[9–11]

Optimum fragmentation from blasts results in reduced costs of both secondary fragmentation and transportation of the blasted rock, effective destressing of rock-burst prone area by creating fracture zone around the potential stress zone to relieve stress, improved environmental aspects as secondary blasting is eliminated. The adverse effect of such blasting i.e., high noise and flyrock are also eliminated, and reductions in energy consumption during crushing and grinding of the ore, as well as improved mineral recovery is achieved through the optimisation process. Controlling both fragmentation and the degree of blast induced damage are important aspects of the project design process in all open excavations, hard rock tunnelling and mining. Poor blasting practices are typified by excessive damage and over-break, oversize fragmentation, restricted access, increased local reinforcement requirements and increased project cycle times and costs. Achieving optimum fragment size not only results in best system performance, but is responsible for minimizing the side effects of blasting like ground vibration, air overpressure, dust, flyrock and overbreak.[6] Therefore, it is essential to study the rock fragmentation by blasting with an aim to achieve the delicate balance between desired fracturing, fragmentation of rock and preventing failure of rock engineering structure under blast loads.[12]

Methods to quantify the size distribution of fragmented rock after blasting are grouped as direct and indirect methods.[13] A comprehensive detail on the blast fragment size measurement methods, tools, applications and drawbacks can be traced to Franklin and Katsabanis.[14] Despite a bias towards the shape of fragments, sieve analysis of fragments is the only direct technique to measure their sizes. Although, being the most accurate technique among others, sieving is not feasible to measure blast fragmentation, because it is expensive, time consuming and involves rehandling of the muck. For this reason, indirect methods, which are observational, empirical and digital in nature have been developed.[15–18]

Fragmentation is measured in terms of mean fragment size (k_{50}) and its uniformity index (n) obtained through a Weibull distribution. However, there have been concerns regarding such distribution pertaining to the assessment of fines. There have been attempts to correct the bias through a new distribution.[19] Empirical methods have been used to assess the degree of fragmentation[20–22] with limitations of the rock characteristics i.e. Rock Mass Description (RMD), Joint Plane Spacing (JPS), Joint Plane Angle (JPA), Rock Density Index (RDI) and Hardness Factor (HF) that are quite subjective in nature and prone to human errors. Digital Image Analysis Technique (DIAT) is one of the most used and accepted method for blast induced fragmentation assessment, in current times[23–28] and has been proven to be an effective tool for blast fragmentation optimization.

In the assessment of blasting results, rapid analysis of muckpile fragmentation is important, so that the fragmentation and muck profile data is acquired and correlated with the productivity of the MMFS. Once the reliability of a blast design has been established, then the blast design can be termed as production pattern. Due to production demands, the muck generated by a blast is available for a short period at the site and a small time-window is available to take measurements of fragmentation. Once the mucking operation starts, there are feeble chances of getting proper data due to several operational reasons. This demands for a rapid fragmentation assessment method.[29] Different image analysis systems like FragScan, Split, Fragalyst and WipFrag are currently in vogue for blast fragmentation analysis with their shortcomings.[30] More recently some advanced methods of fragmentation assessment like Unmanned Arial Vehicles[31], laser-based 3D measurement systems[32] and autonomous methods have been introduced but their efficacy is not yet documented. However, the cost of the modern and advanced versions of *DIAT* systems will be a major constraint for their implementation. Some software(s) like Fragalyst have an option to find the in-situ block size of the rock using 3D joint analysis which can be used to work out the comminution index.

Digital image analysis technique involves the following steps:

1. Capturing of representative images of fragmented rock with a known scale at various intervals of mucking.

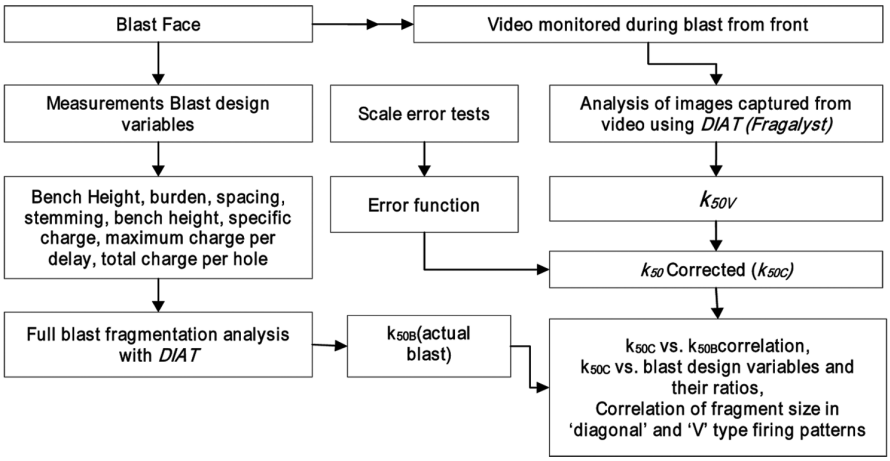

Fig. 1 — Methodology adopted for determination of blast fragmentation and correlations

2. Compilations of the images for different blasts
3. Importing of the images to a digital image analysis software and,

a. Calibration of the images
b. Edge detection
c. Fragment size determination
d. Distribution fitting
e. Mean fragment size and uniformity index
f. Storing of data and further analysis

Keeping in view the shortcomings of the existing fragmentation measurement methods, there is ample scope for innovations in this field. Accordingly, this study reports a new and innovative dynamic digital image analysis technique for rapid analysis of images extracted from videos of blasts monitored from front face. A case study of blast analysis is also provided to augment the concepts and establish the method.

Methodology

The complete methodology of monitoring and analysis of DIAT is provided in Fig. 1. The following steps are involved in the said method:

1. Measurement of blast design variables. This included measurement of bench height at several places along with burden, spacing, stemming, bench height, specific charge, maximum charge per delay, total charge per hole.
2. Tests for checking of error of scale due to movement of broken rock during blasting. A complete description of the method is provided in the following section.
3. Monitoring of video of all the blasts from a distance while focussing on the bench being blasted and keeping the zoom of the camera constant.

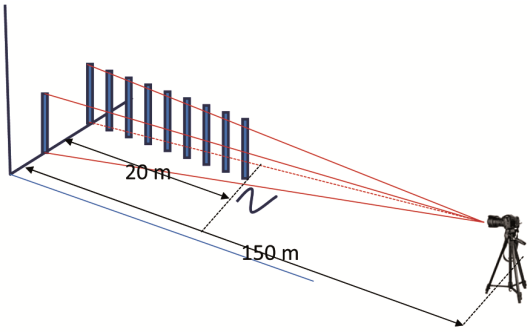

Fig. 2 — Experimental setup for scale correction of the images driven from blast video

4. Derivation of the mean fragment size (k_{50V}) using Fragalyst software of images captured from blast video, and the mean fragment size of the actual blast (k_{50B}) at different stages of mucking operation using Fragalyst software.
5. Correcting the k_{50V} with the correction function due to movement of the muck towards the camera, thus yielding the corrected mean fragment size (k_{50C}).
6. Detailed analysis of the data obtained in terms of relationships of:

a. Mean fragment size (k_{50C}) vs. blast design variables and their ratios.
b. Correlation of fragment size obtained from video (k_{50V}) and that of the actual blast (k_{50B}).
c. Correlation of fragment size in 'diagonal' and '*V*' type firing patterns.

Correction for Movement of Face Being Blasted

In this study, the camera was in a fixed position with a fixed zoom. However, movement of the blast face or fragmented rock towards the camera creates scaling errors. This was resolved by determining the error with the help of an experimental setup (Fig. 2) as explained below:

1. The camera was fixed at a known distance from two calibrators or scales of same size.
2. Considering the throw of the broken rock during blasting i.e., around 20 m, a setup was designed to capture the error due to the movement of the muck observed through images. Accordingly, one of the calibrators was kept fixed and the other one was moved in steps of 2 m up to 20 m towards the camera. In this manner 10 images, with both moving and fixed calibrators visible, were obtained.
3. The images were imported into Fragalyst software wherein the images were calibrated with the help of the fixed scale. Measurements of the size of both the fixed scale and moving scale were taken with the help of a mensuration tool available in the said software. Ratios of the actual and measured distances of the scales were thus registered (Table 1). The throw of the blast was measured and the time steps involved were recalculated for estimating the distance of movement in each frame of the video of the blast. This allowed to calculate the scale effect (Table 1) due to movement of the material towards the camera.
4. The data presented in Table 1 was analysed and revealed the following correction function (Eq. 1) for the movement with distance (Fig. 3) for the camera used in the study.

$$E_s = 0.0349d + 1.0491 \quad \text{... 1}$$

where, E_s is the scale effect for object moving towards the camera and d is the distance of the object with respect to original position i.e., bench or zero position.

Accordingly, the fragment sizes obtained from the blast face images, extracted from the video, were corrected for the scale effects using correction function (Eq. 1) to yield (k_{50C}).

Area of Study

The study was conducted in a limestone mine near Jaipur, India. The data pertaining to different aspects of the mine is compiled in Table 2.

Several blasts were conducted in the above said mines out of which seven full-scale blasts were used to achieve the objectives of this study. Further testing of the method is also proposed in the future studies. The design variables like burden, spacing and stemming, bench height, specific charge, maximum

Table 1 — Test data of correction for movement of the blast face

Distance (m)	Actual object size (m)	Moving object size (m), Measured	Scale effect
0	2.5	2.5	1.00
2	2.5	2.98	1.19
4	2.5	2.89	1.16
6	2.5	3.17	1.27
8	2.5	3.27	1.31
10	2.5	3.56	1.42
12	2.5	3.66	1.46
14	2.5	3.79	1.52
16	2.5	4.17	1.67
18	2.5	4.12	1.65
20	2.5	4.33	1.73

Table 2 — Details of the study site

Sl. No.	Component	Value/description
1	Geology	The Ajabgarh Series of the Precambrian Delhi Super Group
2	Topography	Partly as flat ground and partly hilly terrain with a relief of about 75 m
3	Lithology	Limestone, dolomite, dolomitic limestone and calc-argillaceous rocks
4	General strike direction	NE-SW with variable dip ranging from 44–70° due east
5	Compressive strength of limestone	80 to 110 MPa
6	Production	6 million tonnes per year
7	Explosive	Ammonium Nitrate Fuel Oil with shock tube initiation system with density being 800 kg/cm^3 and average velocity of the detonation of 3700 m/s
8	Firing	Shock tube system anddelaysequencing of 17 ms, 25 msand 42 ms
9	Blast pattern	Staggered
10	Loading operation	Front-end loader, shovel and backhoe
11	Hauling	55 tonne rear dump trucks
12	Bench height	Up to 10 m
13	Burden, spacing, stemming, drill diameter	3.0 m, 3.5 m, 2.5 m, 115 mm, respectively

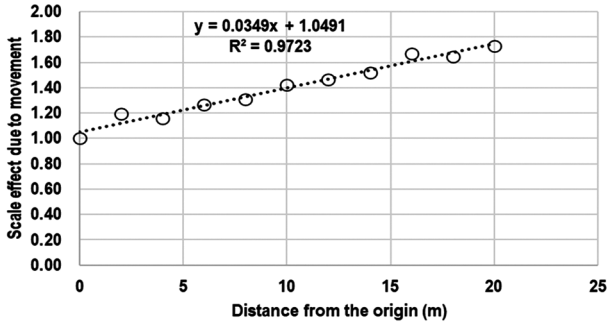

Fig. 3 — Assessment of scale effect due to movement of blast face and rock breakage

charge per delay and total explosive per hole were monitored for such blasts. The explosive was maintained the same for similarity of the design. A high-resolution camera (Make-Nikon, Model – COOLPIX P520, with 42X optical zoom, pixel-18 M, Video – 25 fps) was used to capture entire blast event from the front of the blast from a known distance. The zoom of the video, while monitoring the blast event, was kept constant to avoid scaling errors. The videos of blasts were then processed to extract frames of the blast event at fixed intervals of 0.08 s. All frames that showed proper fragments without obliteration of edges and blur were extracted from the video captured, processed and stored for analysis. An example of such a method is shown in Fig. 4. Throw of the blast was also recorded at the blast sites and used for correction of fragmentation at later stages of the analysis.

The selected frames of all the seven blasts were imported to Fragalyst software. Fragalyst is an image analysis system developed by CSIR-CIMFR (India). The images of blasts face and fragmented material can be imported into the software, calibrated, enhanced and for determination of in situ and blast fragmentation distributions. With the aid of menu-driven software, it is possible to determine the area, size and shape of the fragments in a muck pile. The images of fragments obtained from videos of blasts of seven blasts were processed for edge detection and finally for the determination of mean fragment size (k_{50}). The k_{50} with progressive time was compiled for all the blasts. The data of k_{50} up to around 1.0 s could be processed and showed that there is no further decrease in fragment size beyond 0.56 s. Accordingly, the fragmentation data of all the blasts up to 0.56 s was analysed and is presented here.

In addition, the regular and standard method of determination of mean fragment size (k_{50B}) as mentioned earlier was also conducted for all the blasts. This involved analysis of 25 to 30 images of the complete muck taken at different intervals. This was later used for checking the correlation between the dynamic or video method (k_{50C}) and the fragmentation of the complete muck (k_{50B}).

Results and Discussion

Summary of the data generated thus is presented in Table 3. The k_{50C} presented in the table indicates the mean fragment size at 0.56 s.

Analysis of Fragmentation with Time

The fragmentation data of all the blasts with progressive time was obtained from the images taken at various stages of blast (Table 3) till the

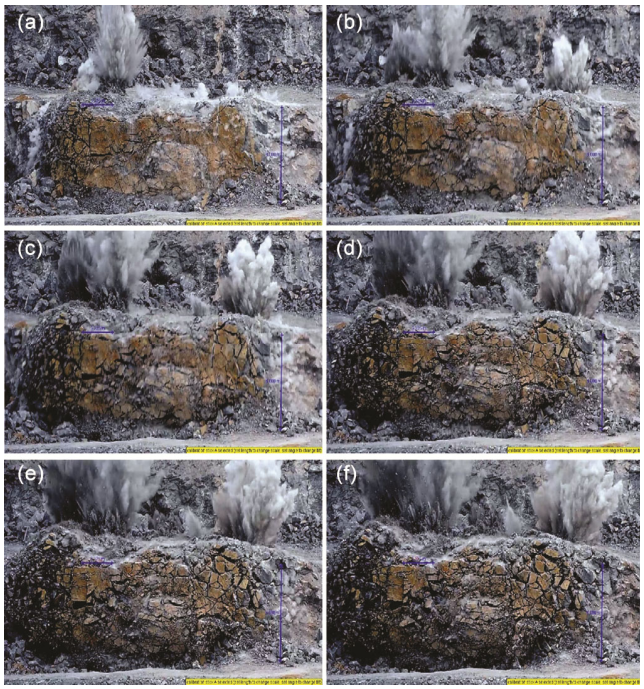

Fig. 4 — Frames of blasting captured at various points during time progression: (a) first breakage visible, (b) 0.08 s, (c) frame 0.16 s, (d) frame 0.32 s, (e) frame 0.48 s, (f) frame 0.56 s

Table 3 — Summary of the data generated

Blast No.	H_b	B	S	l_s	Q	FP	q	k_{50C}	k_{50B}
	m	m	m	m	kg		kg/m^3	m	m
1	8	2.75	3.8	2.7	45	1	0.54	0.56	0.32
2	10	3.00	4.0	2.8	61	1	0.51	0.58	0.28
3	8	2.75	3.9	2.8	44	1	0.52	0.58	0.3
4	8	3.00	4.0	2.8	44	1	0.46	0.86	0.4
5	8	2.40	3.9	2.6	46	2	0.61	0.52	0.18
6	8	2.50	3.8	2.7	45	2	0.59	0.45	0.25
7	8	2.50	3.8	2.4	48	2	0.63	0.36	0.16

Legend: H_b is bench height, B is burden, S is spacing, l_s is stemming length, Q is explosive charge per hole, FP is firing pattern (1 is diagonal and 2 is 'V' type), q is specific charge, k_{50V} is mean fragment size obtained from video images and k_{50C} is corrected mean fragment size using Eq. 1, k_{50B} is mean fragment size obtained from the blast

fragmentation was not further reduced, and the images were clear and not obliterated as shown in Fig. 4. The analysis of fragment size reduction from 0.08 s to 0.56 s for all the blasts is provided in Fig. 5 (a to g). The combined analysis of all the blasts is shown in Fig. 5(h). As explained later, the fragment sizes got reduced with time owing to combination of extension of earlier cracks or generation of fresh cracks by pressurized gas action. It may be noticed that the k_{50C} vs. time correlation yield very high R^2ranging from 0.91 to 0.98.

It can be seen from above Fig. 5 (a to h) that the fragment sizes reduced in a logarithmic manner with progression of time. The analysis revealed that there is no further fragmentation beyond 0.56 s from the point when initial breakage is recorded in the blast or

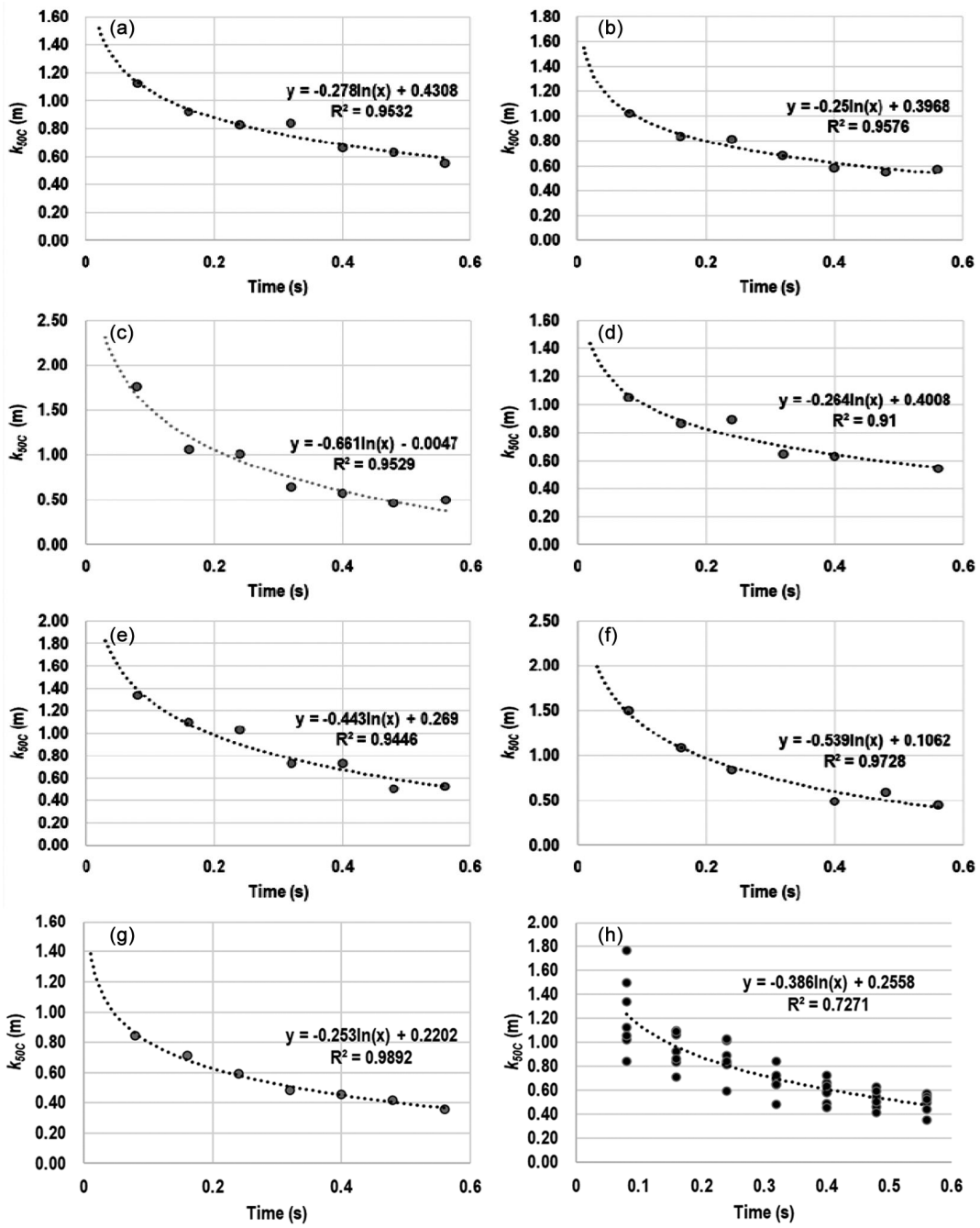

Fig. 5 — (a) k_{50C} vs time for blast 01, (b) k_{50C} vs time for blast 02, (c) k_{50C} vs time for blast 03, (d) k_{50C} vs time for blast 04, (e) k_{50C} vs time for blast 05, (f) k_{50C} vs time for blast 06, (g) k_{50C} vs time for blast 07, (h) k_{50C} vs time for all blasts

the initiation of the fragmentation. The slopes of trends for all the blasts are similar in nature with variation in intercept that can be ascribed to variations in the in-situ block sizes and other variations in rock properties.

The correlation of k_{50C} vs time (Fig. 5 (a to g) of blasts 1 to 7, respectively), show strong relationship with time. The observation is important from fragmentation point of view as the fragment size reduces progressively with time in relation to initial breakage and reveals that there is significant breakage owing to action of gases in the process during the movement of muck. Registration of initial breakage on surface with the movement of the fragments is critical to the analysis as it represents the completion of breakage due to initial shock due to explosive loading.[33]

The percentage reduction of fragment size with time (Fig. 6) as a function of in-situ block size calculated from back calculation yields important information about the blast process and can be used to have a balance in explosive energetics and needs to be seen through further tests.

It can be observed that the data of all the blasts analysed over time shows similar trend, thereby confirming the method. Further controls on firing timing and velocity of detonation of the explosive variations can yield information that can be utilized to fix the firing timings.

Detonation of explosive produces stress wave and large volume of gases at high temperature and pressure and results in breakage of rock through different mechanisms.[34–40] The stress waves produce fresh cracks in rock. It is believed that new crack formation takes place at a particular time. After formation of cracks, cracks expand with time due to high pressure gases and rock particles get detached from rock and are propelled to a distance. Since the initial cracking of the rock is difficult to measure and quantify, the crack expansion continues with further breakage of the fragments in time is demonstrated through this study (Fig. 6).

Calibration with Actual Blast Fragmentation

As mentioned earlier, the fragmentation data of muck pile generated was estimated by image analysis for all the seven blasts. The results were used to develop a correlation between the corrected mean fragment size (k_{50C}) obtained from the dynamics of blast face and the actual blast fragmentation (k_{50B}) measured during mucking as shown in Fig. 7.

It is evident from Fig. 7 that a strong relationship exists between k_{50C} and k_{50B} and thus, k_{50C} can be used to assess the blast fragmentation with a significant degree of reliability.

Blast Design and Fragmentation

The relationships of different blast design variables and their ratios, monitored from the blasts, with the k_{50C} at 0.56 s, are presented in Fig. 8 (a to h). It may be pointed out that number of blasts presented here are representative for demonstration of the efficacy of the methods and the logical trends produced with different blast design variables that is in tune with the objective of this study.

The k_{50C} registers a steady increase with incrase in burden (Fig. 8a), and spacing (Fig. 8b) with increase towards the higher values, increase with increase in stemming (Fig. 8c). Increase in S to B ratio (Fig. 8d) and H_b to B ratio (Fig. 8e) show significant decrease in k_{50C}. The value of S/B ratio of 1.52 gives best k_{50C}. The l_s to B ratio (Fig. 8f) presents mild decrease in k_{50C}. The l_s to H_b ratio (Fig. 8g) though shows a mild increase with its increase and it also presents an optimum trend that points to the fact that an optimum

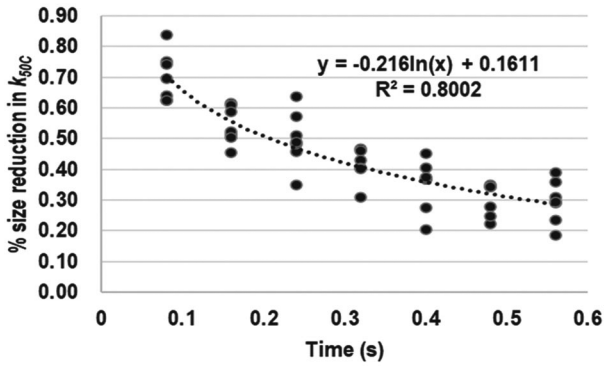

Fig. 6 — Size reduction as function of in-situ block size with time

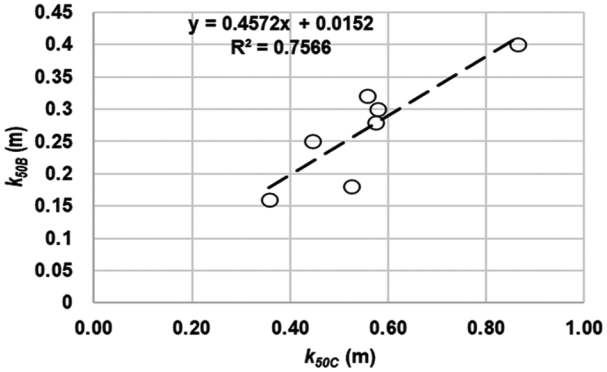

Fig. 7 — k_{50B} of blast vs. k_{50C}measured from video frames

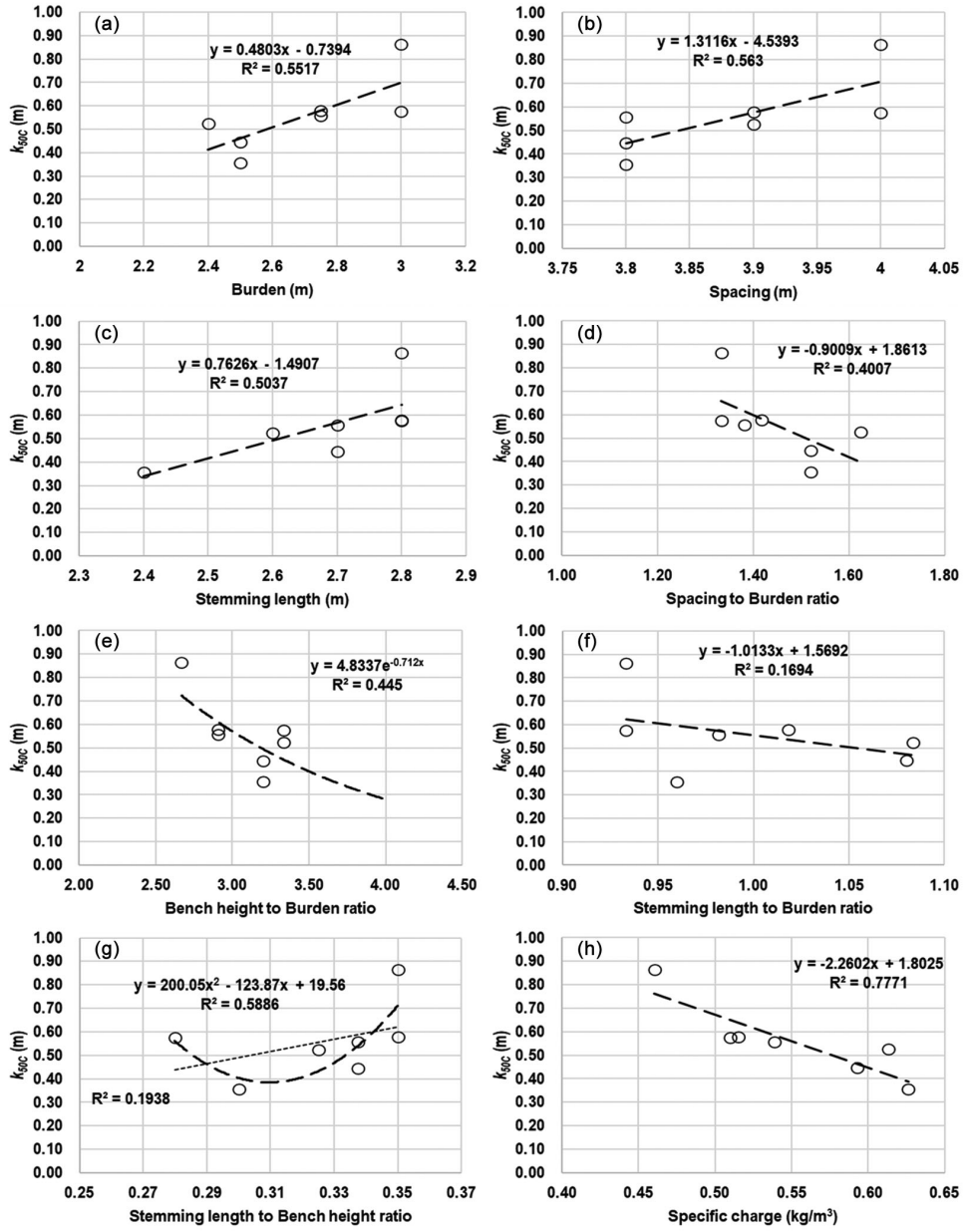

Fig. 8 — (a) k_{50C} vs burden, (b) k_{50C} vs spacing, (c) k_{50C} vs stemming length, (d) k_{50C} vs spacing to burden ratio, (e) k_{50C} vs bench height to burden ratio, (f) k_{50C} vs stemming length to burden ratio, (g) k_{50C} vs stemming length to bench height ratio, (h) k_{50C} vs specific charge

ratio of 0.3 to 0.33 yields best k_{50C}. Specific charge behaves in expected manner as the k_{50C} reduces with increase in q (Fig. 8h).

In addition to the above, the impact on mean fragment size (k_{50C}) due to change in firing pattern from 'diagonal' to '*V*' type was also evaluated (Fig. 9 a & b).

The correlation between 'diagonal' pattern shows a higher k_{50C} in comparision with '*V*' pattern (Fig. 9a) and the relationships show that the differentiation of the fragment size becomes evident after around 0.25 s of the start of initial fragmentation. The difference in intercept is a testimony to the smaller k_{50C} obtained in case of '*V*' pattern (Fig. 9b). This may primarily due to interfragmental collisions. This will need further investigations and validation through further tests in order to define the pure effects of change in firing pattern as this is further controlled by height of fall and velocity of the fragments.

Out of the seven blasts reported in Table 3, four were conducted with 'diagonal' and three with '*V*' type firing patterns. The effective blasting burden

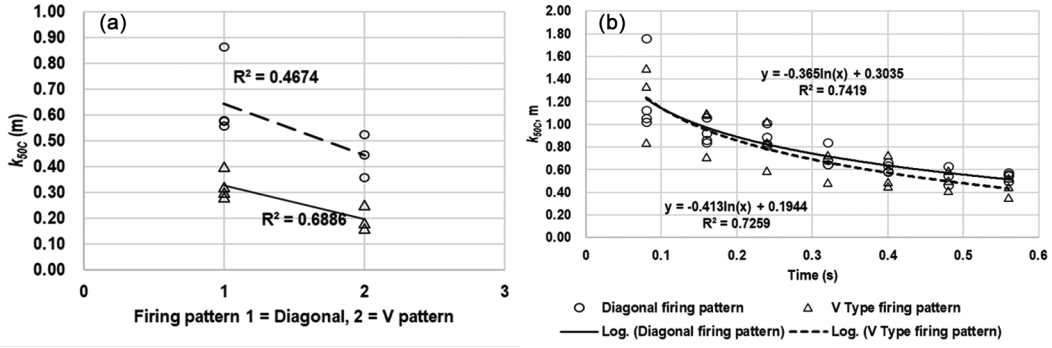

Fig. 9 — (a) Variation of k_{50C} in diagonal and 'V' type firing patterns, (b) Relationships of k_{50C}in diagonal and 'V' type firing patterns

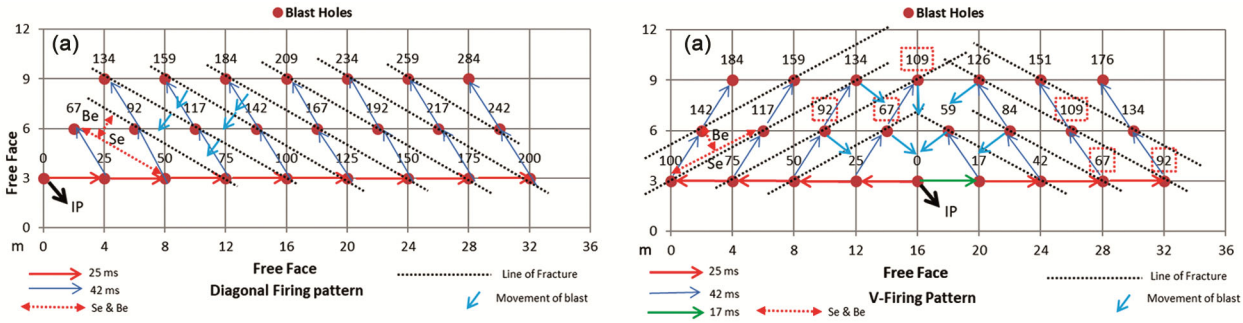

Fig. 10 — (a) Diagonal firing pattern, (b) V-type firing pattern

and spacing, that was actually obtained during firing is also shown in the Fig. 10 (a & b). The calculations of the effective burden and spacing in such cases is explained further.

Diagonal Firing Pattern

In case of diagonal firing pattern, the effective or blasting burden and spacing change with hole-to-hole firing of the blast round. Such condition can be visualized with the help of Fig. 10(a).

A diagonal firing pattern is represented in Fig. 10 (a) in which dotted lines in black colour denote the actual fracture lines while dotted lines in red colour are effective spacing (*Se*) and blue lines the effective burden (*Be*). The *Se* and *Be* in this type of firing pattern can be solved with the help of a parallelogram consisting firing points 25, 50, 92 and 67 in Fig. 10 (a) illustrated with the help of Fig. 11.

The following calculations can thereby made from the Fig. 11:

S = Spacing by side *ab* or *dc*

B = Burden by side *od*

Se = Effective spacing by side *db*

Be = Effective burden

The area of parallelogram (*abcd*) is calculated by

$= ab \times od$

$= S \times B$ ... (2)

The area of this parallelogram also equal to

Area of triangle $\triangle dab$ + $\triangle bcd$

$= \frac{1}{2} (Se \times Be) + \frac{1}{2} (Se \times Be)$

$= Se \times Be$ ... (3)

By Eqs 2 & 3,

$S \times B = Se \times Be$ ...(4)

From $\triangle dob$,

$Se^2 = B^2 + (S+S/2)^2$

$Se = B^2 + 2.25\ S^2$ ... (5)

Now the ratio of *Se*/*Be* can be achieved by replace value of *Be* from Eq. 4,

$Se/Be = Se^2 / (B \times S)$

Replace value of Se^2 from Eq.5,

$Se/Be = B^2 + 2.25\ S^2 / (B \times S)$ ... (6)

With the help of Eqs 4–6 the value of effective burden (*Be*), effective spacing (*Se*) and their ratio (*Se*/*Be*) can be calculated. Such calculations have been used to assess the effective burden and spacing in different firing patterns in present case.

V-type Firing Pattern

The case of V-type firing pattern is similar but has two such limbs of diagonal firing pattern as shown in Fig. 10(b) that can be used to calculate the blasting burden and spacing. From Fig. 10(b) it can be seen that same line of fracture achieved as with diagonal pattern, the result of this *Se*/*Be* ratio will be also same as achieved with diagonal pattern. Many of authors advocate that the V-type firing pattern gives better fragmentation size compared to diagonal firing pattern due to increase in effective spacing (*Se*) to effective burden (*Be*) ratio i.e., increased effective spacing (*Se*) and decreased effective burden *Be*). However, the similarity of fracture lines in both type of firing patterns is not conforming the statement. If a bench has two free faces, then diagonal firing pattern (Fig. 10a) provides two free faces for each blasthole and good fragmentation is achieved. However, if blast face is having only one free face, then V-firing pattern (Fig. 10b) helps to create two free faces for each of the blasthole resulting in good fragmentation. The opposite lines of blast holes collide with each other and induce further rock fragmentation.

The effective spacing to effective burden ratio (m_b) for diagonal and V-type firing patterns as illustrated in Fig. 10 (a & b), are same as line of fractures in both type of patterns are same for similar drill burden and spacing. Accordingly, in order to find out the pure effect of firing patterns on rock fragmentation all other variables have been kept constant in this study (Table 4).

The reduction in fragmentation in the two patterns is from 0.325 to 0.196 cm that corresponds to around 65% reduction in k_{50} in actual blast fragmentation (Fig. 9 a & b). The delays being constant, the difference is k_{50} can be observed from Fig. 9(a) that shows a differentiation in diagonal and V-type firing patterns particularly towards the higher time period (Fig. 9b).

A good relationship between *Se and Be* with k_{50C} can be seen in Fig. 12. Decreasing in value of *Se* and *Be* also decrease in value of k_{50C}. Since, all the variables of the test blasts are constant and the Be and Se are also similar in the both the firing patterns observed the role of collision of fragments in the case of V-type firing pattern assume importance. It is hence concluded that in V-type firing pattern rock collision takes place between holes of opposite direction which results in better fragmentation than the diagonal firing pattern. It also conforms to the finding[41] that if the impacts of the fragments at the time of collision are greater than the strength of the fragments, then these will break on impact.

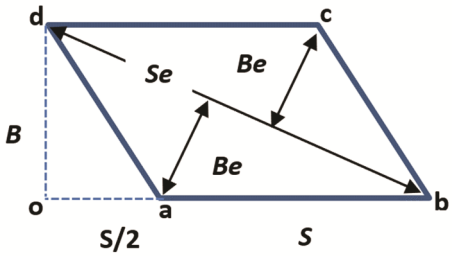

Fig. 11 — Solution for Be and Se using a parallelogram geometric method

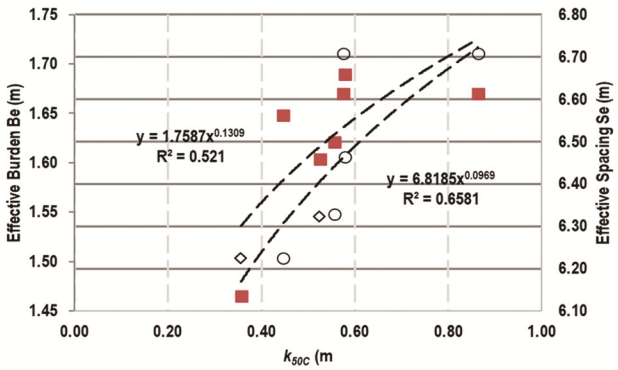

Fig. 12 — k_{50C} vs. Effective burden Be and Effective Se

Table 4 — Effect of firing pattern on mean fragmentation size (k_{50c})

Sl.No.	Blast ID	H_b (m)	B (m)	S (m)	ls (m)	Firing Pattern	Mb	Se (m)	Be (m)	k_{50C} (m)	Delay ms/m of Se	Delay ms/m of Be
1	022	8	2.75	3.8	2.7	Diagonal	3.90	6.33	1.62	0.56	3.95	25.91
2	029	10	3	4	2.8	Diagonal	4.02	6.71	1.67	0.58	3.73	25.16
3	057	8	2.75	3.9	2.8	Diagonal	3.83	6.46	1.69	0.58	3.87	24.86
4	063	8	3	4	2.8	Diagonal	4.02	6.71	1.67	0.86	3.73	25.16
5	315	8	2.4	3.9	2.6	V-type	3.94	6.32	1.60	0.52	3.95	26.19
6	355	8	2.5	3.8	2.7	V-type	3.78	6.22	1.65	0.45	4.02	25.48
7	001	8	2.5	3.8	2.4	V-type	4.25	6.22	1.47	0.36	4.02	28.66

Mb is ratio of Se to Be, Se is effective spacing, Be is effective burden

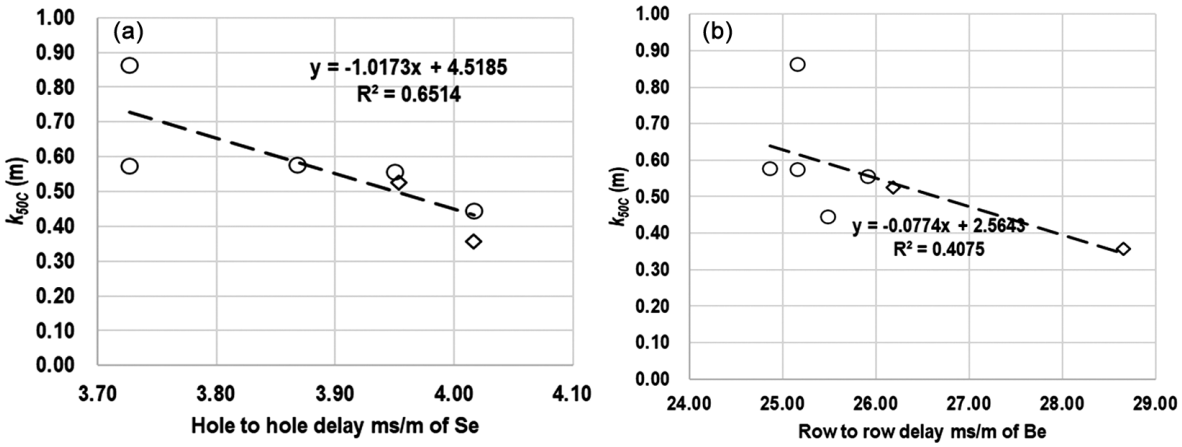

Fig. 13 — (a) k_{50C} vs Hole-to-hole delay ms/m of Se, (b) k_{50C} vs Row-to-row delay ms/m of Be

Also, the delays in both the patterns are similar that show a better fragmentation at a hole-to-hole delay of 4 ms/s of *Se* and row-to-row delay of 28 ms/m of *Be* and hence provides a basis for selection of delays (Fig. 13 a & b). However, millisecond delay tests with use of electronic detonator will provide a better insight into the delay selection. A possible impact of hole to hole and row to row delay is explained in Fig. 13 (a & b) that point to the fact that there is a decrease in fragment size with increase in delay. However, this will require further investigation.

The surface plot using multiple linear regression of k_{50C} with time and specific charge (Fig. 14) shows that higher interaction time with gas pressure and higher specific charge collectively contributed to reduction in fragment size. More time of interaction is seen in case of V-type firing pattern when compared to diagonal pattern.

Assuming that initial stages of the time represent the in-situ block size (*IBS*), it can be observed from Fig. 14 that at lower specific charge for higher *IBS*, the reduction in fragmentation is initially steep, while the case is different with higher specific charge. This indicates that the fragmentation commences quite ahead and manifests on surface at a later stage.

Comparison with Existing Methods

A new yet innovative method to assess the blast fragmentation from videos of blast is introduced here. The data acquired and analysed is based on limited studies in a limestone mine. A comparison of the method introduced with the existing *DIAT* method is provided in Table 5. The data pertaining to time domain is based on experience of fragmentation analysis conducted by the authors.

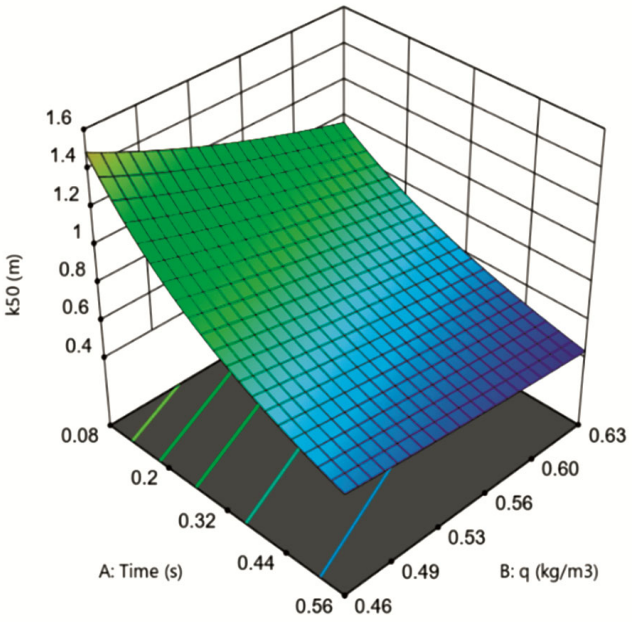

Fig. 14 — Response surface of k50 with specific charge and time

The H_b to B ratio (Fig. 8e) when extrapolated conforms to the accepted norm[42] that increase in the ratio beyond 4 will not yield further improvements in fragmentation.

The impact on mean fragment size due to change in firing pattern from 'diagonal' to '*V*' type was also evaluated (Fig. 9 a & b) which revealed that '*V*' type firing pattern yields finer k_{50C} in comparison to the diagonal type. This may primarily be due to inter-fragmental collisions. This will need further investigations and validation through further tests. With such analysis it is also possible to have an idea of obtaining better fragmentation using suitable delays.

Table 5 — Comparison of the new method introduced with the existing methods

Sl. No.	Criterion	Existing methods	Method introduced in this paper
1.	Time taken to get muck images	Full blast cycle	Just blast video of few seconds
2.	Time taken to analyse images	100 minutes per blast	10 minutes for image extraction 40 minutes for image analysis
3.	Reporting	Varies with analysis software	10 minutes with Fragalyst
4.	Requirements	All blasts need to be measured	Video of all blasts and one full blast analysis
5.	Manpower	Two persons required	Half man day invested
6.	Safety	May not be safe while equipment(s) are in operation	Completely safe
7.	Others	Images are post blast in nature, hence do not reflect impact of rockmass	Video can be used for complete blast analysis including effect of rockmass
8.	Analysis	Only fragmentation can be assessed	Reduction of fragment size with time, possibility of in-situ block size estimation and timing effects and nature of fracturing can be captured.

Conclusions

This study introduces a new and fast method to determine the blast induced fragmentation in mines. The suggested approach allows to measure the mean fragment sizes from blast images derived from a video of the front face breakage, that in turn are comparable with that of complete muck of the blasts. Blast fragmentation can be assessed with the help of videos of a blast face using calibration with the fragmentation in actual blast muck. The reduction of in situ block size with time from initiation of the blast using images extracted from blast video with particular time intervals can be worked out with this method. This method demonstrates the effective use of DIAT in such analysis. Based on the fragment sizes obtained, blasting parameters can be re-designed to obtain the optimum results. The method provides a means to determine the progress of fragmentation with time and can be utilized to design the timing of hole delays. It was also demonstrated that the V-type firing pattern yields significantly better fragmentation than the diagonal type.

This method is expected to save considerable time and resources in blast fragmentation assessment as it is direct yet simple in application. This method also presents a possibility of estimation of in situ block size of the rock being blasted. The fragment sizes also correlate well with the blast design variables and their ratios and hence can be used in blast design evaluation. The method also helps in defining the timing sequence of blast holes for achieving optimum fragment size.

The drawback of this method is that it provides rock fragmentation of only that portion of rock which is captured by camera. However, with the help of calibration factor obtained from full scale blast fragmentation measurement, it can give good result for fragmentation assessment of the blasts. A possibility of inherent errors due to image analysis in the method introduced cannot be ruled out. However, these errors are systemic and common to individual analysis and can be ignored. There is a scope to improve the measurements further in terms of validation and perfection of the method. Further studies can consolidate the approach for wider use and acceptability.

Acknowledgements

The paper forms a part of the PhD work of the first author. The authors are thankful to their respective employers for their permission to publish the findings. Help of several persons in conducting the study is duly acknowledged.

Conflict of Interest

The authors declare that there is no conflict of interest to disclose.

References

1 Seccatore J, A review of the benefits for comminution circuits offered by rock blasting, *Rev Esc Minas*, **72/1 (**2019) 141–146, doi:10.1590/0370-44672017720125

2 Hustrulid W, *Blasting Principles for Open Pit Mining: Volume 1 - General Design Concepts*, (AA Balkema Rotterdam) **1 (**1999) 24–61.

3 Mackenzie A, Cost of explosives—do you evaluate it properly? *Min Congr J*, **52/5 (**1966) 32–41.

4 Božić B, Control of fragmentation by blasting, *Rud Geol Naft Zb*, **10/1** (1998) 49–57.

5 Kanchibotla S S, Valery W & Morrell S, Modelling fines in blast fragmentation and its impact on crushing and grinding, in *Explo '99–A Conf Rock Breaking*, The Australasian Institute of Mining and Metallurgy, Kalgoorlie, Australia, (1999) 137–144).

6 Da Gama C D & Jimeno C L, Rock fragmentation control for blasting cost minimization and environmental impact abatement, *Proc Rock Fragmentation by Blasting*, FRAGBLAST (1993) 273–280.

7 Shim H J, Ryu D W, Chung S K, Synn J H & Song J J, Optimized blasting design for large-scale quarrying based on a 3-D spatial distribution of rock factor, *Int J Rock Mech Min Sci*, **46/2** (2009) 326–332, doi:10.1016/j.ijrmms.2008.07.006.

8 Afeni T B, Optimization of drilling and blasting operations in an open pit mine-the SOMAIR experience, *Min Sci Technol*, **19/6** (2009) 736–739, doi:10.1016/S1674-5264(09) 60134-4.

9 Chakraborty A K, Ramulu M, Raina A K, Choudhury P B, Haldar A, Sahu P B & Bandopadhyay C, Rock fragmentation system analysis applying cause-effect relationship, *J Mines Met Fuels*, **3-4** (2005) 47–54.

10 Chakraborty A K, Raina A K, Ramulu M, Choudhury P B, Haldar A, Sahoo P & Bandopadhyay C, Development of rational models for tunnel blast prediction based on a parametric study, *Geotech Geol Eng* **22/4** (2004) 477–496, doi:10.1023/B:GEGE.0000047042.90200.a8

11 Raina A K, Ramulu M, Choudhury P B, Chakraborty A K, Sinha A, Ramesh-Kumar B & Fazal M, Productivity improvement in an opencast coal mine in India using digital image analysis technique, in *Rock Fragmentation by Blasting - Proc 9th Int Symp Rock Fragmentation by Blasting*, *FRAGBLAST 9* (2010) 707–716.

12 An H M, Liu H Y, Han H, Zheng X & Wang X G, Hybrid finite-discrete element modelling of dynamic fracture and resultant fragment casting and muck-piling by rock blast, *Comput Geotech*, **81** (2017) 322–345, doi:10.1016 /j.compgeo.2016.09.007.

13 Raina A K, Blast fragmentation assessment and optimization: Back to basics, *J Mines Met Fuels*, **61/7-8** (2013) 207–212.

14 Franklin J A & Katsabanis T *Measurement of Blast Fragmentation*, Balkema, Rotterdam (1996).

15 Yang X, Ren T & Tan L, Size distribution measurement of coal fragments using digital imaging processing, *Meas J Int Meas Confed*, **160** (2020) 107867, doi:10.1016/ j.measurement.2020.107867.

16 Engin I C, Maerz N H, Boyko K J & Reals R, Practical measurement of size distribution of blasted rocks using lidar scan data, *Rock Mech Rock Eng*, **53/10** (2020) 4653–4671, doi:10.1007/s00603-020-02181-5.

17 Jiang Z D, Wang Q B, Adhikari K, Brye K R, Sun Z X, Sun F J & Owens P R, A vertical profile imaging method for quantifying rock fragments in gravelly soil,*Catena*, **193** (2020), doi:10.1016/j.catena.2020.104590.

18 Jethro M A, Ajayi O D & Elijah O P, Rock fragmentation prediction using Kuz-Ram model, *J Environ Earth Sci*, **6/5** (2016) 110–115.

19 Ouchterlony F, The Swebrec© function: linking fragmentation by blasting and crushing, *Inst Min Metall Trans Sect A Min Technol*, **114/1 (**2005) 29–44, doi:10.1179/037178405X44539.

20 Cunningham C V B, The Kuz-Ram model for prediction of fragmentation from blasting, *Proc 1st Int Symp Rock Fragment Blast* (1983) 439–453.

21 Dondov E, Chen G & Dendev N, Analysis and evaluation of fragment size distributions in rock blasting at the Erdenet copper mine, In *53rd U S Rock Mechanics/Geomechanics Symposium*, New York, 2019, 1618.

22 Strelec S, Gazdek M & Mesec J, Blasting design for obtaining desired fragmentation, *Teh Gazette*, **18/1** (2011) 79–96.

23 Lowery M A, Kemeny J & Girdner K, Advances in blasting practices through the accurate quantification of blast fragmentation, *Min Eng*, **53/10** (2001) 55–61.

24 Chi X, Zhao X & Cui W, Judgment and evaluation system of 3D-suface blasting based on GIS, in *Proc - 2010 3rd IEEE Int Conf Comput Sci Info Technol*, *ICCSIT 2010*, **2** (2010) 197–200, doi:10.1109/ICCSIT.2010.5563801.

25 Palangio T W, Palangio T C & Maerz N H, Advanced automatic optical blast fragmentation sizing and tracking, *EFEE Conf Proc Bright*, (2005) 259–267, https://mospace.umsystem.edu/xmlui/handle/10355/31807.

26 Siddiqui F, Shah S & Behan M. Measurement of size distribution of blasted rock using digital image processing, *J King Abdulaziz Univ Sci*, **20/9** (2009) 81–93, doi:10.4197/eng.20–2.4.

27 Choudhary B S & Rai P, Stemming plug and its effect on fragmentation and muckpile shape parameters, *Int J Min Miner Eng*, **4/4**(2013) 296–311, doi:10.1504/ IJMME.2013.056854.

28 Raina A K, Choudhury P B, Ramulu M, Chakraborty A K, Dudhankar A S, Udpikar V, Ghatpande N & Misra D D, FRAGALYST - An indigenous digital image analysis system for grain size measurements in mines, *J Geol Soc India*, **59/6** (2002) 561–569.

29 Ozkahraman H T, Fragmentation assessment and design of blast pattern at Goltas limestone quarry, Turkey, *Int J Rock Mech Min Sci*, **43/4** (2006) 628–633, doi:10.1016/ j.ijrmms.2005.09.004.

30 Sudhakar J, Adhikari G R & Gupta R N, Comparison of fragmentation measurements by photographic and image analysis techniques, *Rock Mech Rock Eng*, **39/2** (2006), doi:10.1007/s00603-005-0044-9.

31 Bamford T, Esmaeili K & Schoellig A P, A real-time analysis of post-blast rock fragmentation using UAV technology, *Int J Mining Reclam Environ*, **31/6** (2017) 439–456, doi:10.1080/17480930.2017.1339170.

32 Thurley M J, Wimmer M & Nordqvist A, Blast fragmentation measurement based on 3D imaging in sublevel caving draw-points and LHD buckets at LKAB Kiruna, *Int Symp Rock Fragm by Blasting*, (2015) 763–774.

33 Zhang Y Q, Hao H & Lu Y, Anisotropic dynamic damage and fragmentation of rock materials under explosive loading, *Int J Eng Sci*, **41/9** (2003), doi:10.1016/S0020-7225(02)00378-6.

34 Zhu Z, Mohanty B & Xie H, Numerical investigation of blasting-induced crack initiation and propagation in rocks, *Int J Rock Mech Min Sci*, **44/3** (2007) 412–424, doi:10.1016/j.ijrmms.2006.09.002.

35 Kutter H K & Fairhurst C, On the fracture process in blasting, *Int J Rock Mech Min Sci*, **8/3**(1971) 181–202, doi:10.1016/0148-9062(71)90018-0.

36 Ning Y, Yang J, An X & Ma G, Modelling rock fracturing and blast-induced rock mass failure via advanced discretisation within the discontinuous deformation analysis framework, *Comput Geotech*, **38/1**(2011) 40–49, doi:10.1016/j.compgeo.2010.09.003.

37 Jeong H, Jeon B, Choi S & Jeon S, Fracturing behavior around a blasthole in a brittle material under blasting loading, *Int J Impact Eng*, **140** (2020) 103562, doi:10.1016/j.ijimpeng.2020.103562.

38 Rossmanith H P, Daehnke A, Knasmillner R E, Kouzniak N, Ohtsu M & Uenishi K, Fracture mechanics applications to drilling and blasting, *Fatigue Fract Eng Mater Struct*, **20/11** (1997), doi:10.1111/j.1460-2695.1997.tb01515.x.

39 Duvall W I & Atchison T C, *Rock Breakage by Explosives*, **5356** (1957) 52.

40 Cunningham C V B, Concepts of blast hole pressure applied to blast design, *Fragblast*, **10/1-2** (2006) 33–45, doi:10.1080/13855140600852977.

41 Chouhan L S & Raina A K, Analysis of in-flight collision process during V-type firing pattern in surface blasting using simple physics, *J Inst Eng Ser D*, **96/2** (2015) 85–91, doi:10.1007/s40033-015-0076-6.

42 Konya C J & Walter E J, *Rock Blasting And Overbreak Control, United States. Federal Highway Administration Report No. FHWA-HI-92-001, NHI-13211,*(1991) 430p.